Spectroscopy of triply and quadruply ionized states of mercury

M. Huttula,[1,2,3,*] S.-M. Huttula,[1,2,3] P. Lablanquie,[1,2] J. Palaudoux,[1,2] L. Andric,[1,2,4] J. H. D. Eland,[5] and F. Penent[1,2]

[1]*Laboratoire de Chimie Physique-Matière et Rayonnement, Université Pierre et Marie Curie, 11 rue Pierre et Marie Curie, F-75231 Paris Cedex 05, France*

[2]*CNRS, Laboratoire de Chimie Physique-Matière et Rayonnement (UMR 7614), 11 rue Pierre et Marie Curie, F-75231 Paris Cedex 05, France*

[3]*Department of Physics, P.O. Box 3000, University of Oulu, FIN-90014 University of Oulu, Finland*

[4]*Université Paris–Est, 5 boulevard Descartes, F-77454 Marne-la Vallée Cedex 2, France*

[5]*Department of Chemistry, Physical and Theoretical Chemistry Laboratory, Oxford University, South Parks Road, Oxford, OX1 3QZ, United Kingdom*

(Received 20 January 2011; published 25 March 2011)

Multielectron coincidence spectroscopy has been used to study multiple ionization of atomic mercury. The binding energies of triply and quadruply ionized states of Hg have been determined from three- and fourfold electron coincidences. Relativistic *ab initio* theory has been used to calculate the state energies and predict the experimental findings.

DOI: 10.1103/PhysRevA.83.032510 PACS number(s): 32.30.−r, 32.80.Fb, 32.80.Aa, 31.15.A−

I. INTRODUCTION

Electron spectroscopy is a well-established method for studies of electronic structure in various forms of matter. Since the pioneering implementation of "high-resolution" electron spectroscopy in the 1960s [1,2], continuous improvements in the experimental techniques for electron detection, in the sources for excitation, and in energy resolution on both sides, have been made. Currently, third-generation synchrotron radiation sources and multielectron coincidence setups are common tools for experimentalists. The magnetic bottle multielectron coincidence apparatus developed by Eland *et al.* [3] was implemented for use with synchrotron radiation (SR) [4] and has been applied to studies of multiple photoionization in various gas phase atoms and molecules (see, for instance, Refs. [5–10]). Because of the need of an evaporation source to produce vapor phase targets and also on account of the increasingly complex spectra from open-shell systems, SR electron coincidence studies following core ionization of metal atoms are still rare, although the field is well established and is in constant development in conventional electron spectroscopy (see, e.g., Refs. [11–13]).

Mercury is a liquid metal at room temperature, with an electronic configuration of filled $4f$, $5d$, and $6s$ orbitals outside a xenon structure ([Xe]$4f^{14}5d^{10}6s^2$). A comprehensive study of mercury photoionization with a comparison of spectra between solid and vapor phase was done by Svensson *et al.* [14] in 1975 using Al $K\alpha$ radiation. $4f$, $5p$, and $5d$ subshell photoionization was further studied by Kobrin *et al.* with determinations of relative cross sections, branching ratios, and photoelectron angular distributions [15]. The Auger decay of the $4f$ core hole to the $5d^{-2}$ configuration was studied by Aksela *et al.* in 1977 [16]. Studies of the ionized states of mercury date back to the 1960s [17], when cross sections for single and double photoionization were reported. The valence $6s$ and inner valence $5d$ ionizations leading to singly and doubly ionized states of mercury were most recently studied by Eland *et al.* [18] in 2004. They performed multicoincidence studies with a pulsed He discharge light source with a focus on the double ionization up to 48 eV (He IIβ) in binding energy. Their study demonstrates nicely the ability of a time-of-flight (TOF) electron-electron coincidence method to reveal the doubly ionized states of an atom directly and accurately.

Although Hg has been widely studied, the only existing report on the binding energies of triply ionized states is given in the optical data compilation by Moore [19] providing the ionization limit and a few observed and some extrapolated triply ionized states. For the quadruply ionized (Hg^{4+}) states no reports on the binding-energy positions were found to exist. The distribution of the Hg^{3+} and Hg^{4+} ionized states has, however, been studied by optical spectroscopy for transitions between defined electronic states, for triply ionized states by Joshi *et al.* [20] and van der Valk *et al.* [21], and by Raassen [22] and Wyart [23] for quadruply ionized states. These authors have also made extensive least-square-fitting types of semiempirical calculations with the objective of reliable identification of the energy states and correlation. In the present work, the multiply ionized states of mercury have been studied experimentally, applying multielectron coincidence spectroscopy together with SR excitation to metal vapor studies. The binding energies of triply and quadruply ionized states of mercury directly observed are presented. The observations are compared to the predictions by relativistic fully *ab initio* multiconfiguration Dirac-Fock calculations.

II. EXPERIMENTS

The experiments were carried out at the Bessy-II storage ring synchrotron radiation source in Berlin. The magnetic bottle multielectron coincidence spectrometer, described in Ref. [5], was used at the spherical grating monochromator beamline U 125/2, where the energy range extends from 29 to 400 eV. To accommodate the relatively long TOF of the electrons (up to 5 μs for the slowest electrons that were accelerated into the TOF tube by a ~ -0.5 V repelling potential applied on the magnet), a specially designed chopper [10,24,25] was used to decrease the single bunch pulse

*marko.huttula@oulu.fi

frequency $f = 1.25$ MHz ($T = 800.5$ ns) of the storage ring to an 80 kHz pulse repetition rate, whereby the light pulse period was expanded to ∼12.5 μs to allow absolute TOF measurements as the electron TOF can be longer than the single bunch period of 800.5 ns. The photon pulses going through the chopper are detected by a channeltron electron multiplier directly inserted into the photon beam path at the end of the vacuum chamber. This signal is used to select the precise ring clock signal relating to the light pulse causing ionization and thus allows absolute TOF determination independent of any jitter on the channeltron signal. Electron times of flight are measured by a time to digital converter (TDC) with a 250 ps resolution. The TDC acquisition procedure is initiated by the detecton of a first electron, which opens a gate for 8 μs during which the arrival times of successive electrons and of the (delayed) ring pulse signal are measured. The electrons' times of flight are determined as the time difference between their arrival and the light pulse. Photon energy calibration of the monochromator was performed by measuring the total electron yield of He doubly excited states below the He^{2+} threshold, with the magnetic bottle. The TOF to kinetic energy calibration of the magnetic bottle was performed by measuring the $N = 2$ photoelectron satellite line of helium at a number of kinetic energies starting from 200 meV. The helium $N = 1$ line was used for kinetic energies above 40 eV. The extrapolated position of zero kinetic electrons (visible, for instance, in He double photoionization) was also taken into account in the calibration. This calibration was cross-checked with the positions of the double-ionized states of mercury, where the $5d^8 6s^2(^1S_0)$ state was taken to be at 48.90 eV binding energy [19]. Small energy shifts induced by different experimental conditions (e.g., deposition of mercury in the chamber inducing contact potentials) were corrected as constant energy shifts using a strong autoionization Auger line $5d^9_{3/2}6p^2(^1S_0) \rightarrow 5d^{10}(^1S_0)$ of excited mercury atoms as an autocalibration point for low kinetic energy. We find this line, assigned as A in Fig. 1, located at 0.55 eV kinetic energy, being well in line with the values of 0.54 and 0.59 eV evaluated from the binding-energy values reported by Eland and Feifel [18]. The binding energies of the first triple-ionized states, shown as the inset, were resolved from the same dataset as the calibration spectrum presented in Fig. 1, providing the most reliable calibration. The detection efficiency for electrons from 0 to 200 eV was found to be more than 55%, allowing for the effective detection of three and four electrons in coincidences. In order to avoid any significant contribution of random coincidences, the electron count rate was limited to between 1 and 3 kHz.

III. CALCULATIONS

In order to find tentative interpretations of the observed structures of the ionic states of atomic Hg, fully *ab initio* calculations were performed. The energies and eigenvectors were calculated for triply and quadruply ionized states using the relativistic Dirac-Fock method. The GRASP92 [26] package was used to solve the radial wave functions of the one-electron spin orbitals. The atomic state functions (ASF) for bound states were obtained by diagonalizing the Hamiltonian matrix in the basis of JJ-coupled antisymmetric configuration state

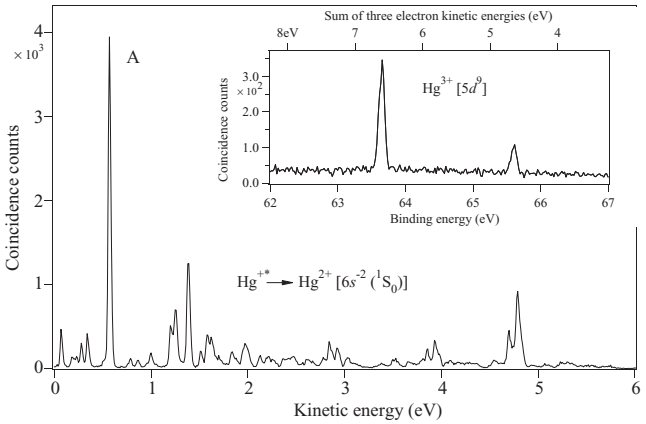

FIG. 1. The population of the energetically lowest double ionization state of mercury plotted as intensity along a constant energy sum of two electron energies. The inset presents the lowest binding-energy triply ionized states as energy sums of all three electron events. The two spectra are derived from the same dataset measured using 70 eV photon energy.

functions with the RCI program [27,28]. The optimization of the radial wave functions was performed in the average level scheme in which the orbitals were optimized by minimizing the average energy of the ASF. In comparison to the least-square-fitting calculations presented with the optical experiments in Refs. [20–23], our predictions provide a completely *ab initio* approach with included relativistic effects. The applied JJ coupling scheme could be expected to provide a more natural approach for a heavy atomic mass case of Hg in comparison to the LS coupling.

As is shown in previous studies, the ground state of the atom is best described as a mixed configuration including a high contribution of $5d^{10}6p^2$ and also small amounts of $5d^{10}7s^2$ and $5d^{10}6d^2$ configurations [18]. In the present work, a single configuration approximation was used for the ground state of mercury including only the nonrelativistic $[Xe]4f^{14}5d^{10}6s^2$ configuration. The approach has no influence on the indentification of the ionized states but it may slightly change the predicted absolute binding energies, which are taken as energy differences of the ground and ionized states. For triply and quadruply ionized states, multiconfiguration calculations including nonrelativistic configurations $5d^9$, $5d^8 6s^1$, $5d^7 6s^2$ and $5d^8$, $5d^7 6s^1$, $5d^6 6s^2$ were performed, respectively.

IV. RESULTS AND DISCUSSION

The multielectron coincidence data of the magnetic bottle experiment consist of a list of events corresponding to the absolute TOF of all the electrons generated by a light pulse. Since the TDC is launched by the detection of a first electron, every event consists of the detection of at least one electron; up to n electrons are recorded in n-fold multiple ionization. The analysis of the data was done using the igor macro package developed in the Laboratoire de Chimie Physique-Matiere et Rayonnement (LPC-MR) [29]. Events with detections of two, three, and four electrons were selected from experiments performed at several photon energies to represent the formation of doubly, triply, and quadruply ionized states of the mercury atom. For the selected events the summation of the electron

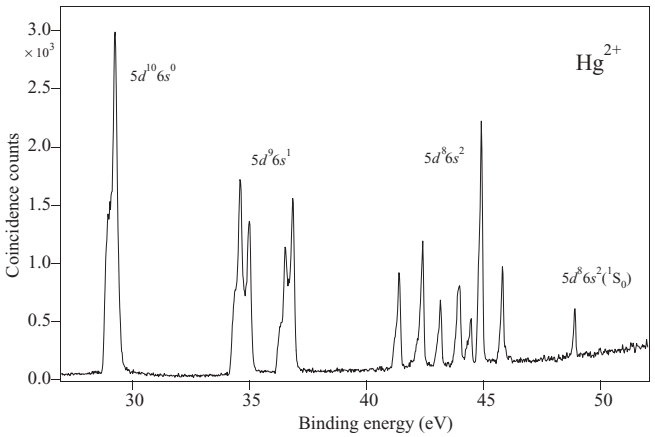

FIG. 2. Energy sum of electron pairs at the photon energy of 60 eV. The identification of the double-ionized states is based on Refs. [19] and [18].

energies equals the available kinetic energy and thus, with the known photon energy, the binding energy of a chosen ionic state. The kinetic-energy resolution of the magnetic bottle spectrometer is best close to zero kinetic energy and rapidly deteriorated at higher kinetic energies ($\Delta E/E \sim 1.6\%$). Thus data were collected with several photon energies from 60 to 180 eV to optimize energy resolutions for double, triple, and quadruple ionizations and to check the evolution of the population of the accessible states.

The experimental spectra showing doubly, triply, and quadruply ionized states of free mercury atoms are presented in Figs. 2, 3, and 4, respectively. The doubly ionized states presented in Fig. 2 were measured at a photon energy of 60 eV and were mainly used to reevaluate the TOF to kinetic-energy conversion of the spectrometer. The doubly ionized states were found to resemble the spectra presented in Ref. [18] with an additional $5d^8 6s^2(^1S_0)$ state at the binding energy of 48.90 eV [19], which lies above the photon energy of the previous experiment.

In order to examine triply ionized states over a wide energy range, three different photon energies were used. First, the

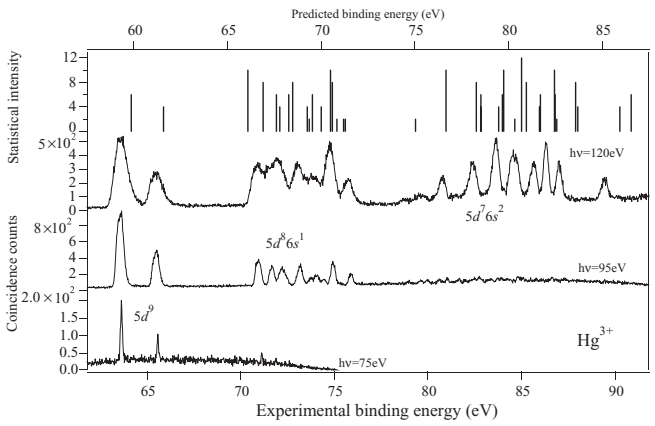

FIG. 3. Energy sum of triple electron-electron event combinations presenting the triple-ionized states of Hg. For the line numbers, refer to Table I. The vertical bars represent the calculated energy positions.

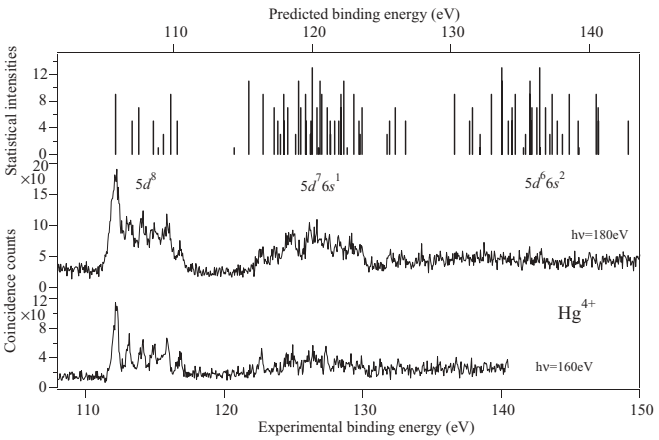

FIG. 4. Energy sum of four electron-electron event combinations presenting the quadruple-ionized states of Hg. For the line numbers, refer to Table II. The vertical bars represent the calculated energy positions.

$5d^9(J = 5/2)$ state, i.e., the triple-ionization threshold of mercury, was measured at the photon energy of 75 eV to have a good energy resolution. Next, the triply ionized states up to 73 eV in binding energy (see Fig. 3) were recorded at a photon energy of 95 eV. Finally, the high binding-energy group of Fig. 3 was measured at a photon energy of 120 eV in order to acquire a higher relative number of spectral events. Although the binding energies of triply ionized states of $5d^7 6s^2$ configuration are already exceeded at a photon energy of 95 eV, the states are not efficiently populated. The photon energy of 120 eV is, on the other hand, just above the $4f^{-1}$ core ionization threshold and thus can provide intensity for the Hg^{3+} group of states through an Auger decay. The threshold of triply charged Hg^{3+} is determined using 70 eV photon energy (see Fig. 1) to be at 63.65 eV $\pm$ 70 meV. By comparison, the NIST compilation [30] and Moore's tables [19] give an estimate of the Hg^{3+} threshold as being around 63.4 eV.

The calculated energy positions of the Hg^{3+} states are presented as vertical bars in Fig. 3. The length of the bars represents the relative $2J + 1$ statistical weight of the levels within each final state group defined by the configuration. The triply ionized states were assigned by comparison with the theoretical predictions. The identifications are presented in Table I together with experimental and predicted binding energies. The assignments are given in the $J\,J$ coupling scheme with one or two leading terms of atomic state function. The experimental error estimate of 70 meV arises mainly from uncertainty in the absolute energy calibration of the spectra, which is around 20 meV for a single-electron energy leading to 60 meV for a sum of three electron energies. An additional 10 meV comes from the peak-fitting procedure. The identification of the spectral lines was compared to the optical data presented in Moore's table [19] but the correspondence was found to be weak. Whereas the optically tabulated values begin from $5d^8 6s(^4F_{3/2,5/2,7/2,9/2})$ states, we clearly observe the two $5d^9(J = 5/2,3/2)$ components (Fig. 1, inset) at the lowest energy. The spin-orbit splitting for $5d$ is given as 1.01 eV by the optical data, while our theoretical prediction agrees very well with the observed value of 1.93 eV. The development of the lowest binding-energy triply ionized configuration from

TABLE I. Experimental and calculated binding energies and identification of triply ionized states of Hg.

Peak	Binding energies (eV) Expt.	Calc.	Identification	
1	63.65 ± 0.07	59.86	$99\%5d^4_{3/2}5d^5_{5/2}, J = 5/2$	
2	1.93	1.72	$99\%5d^3_{3/2}5d^6_{5/2}, J = 3/2$	
3	7.41	6.22	$92\%5d^4_{3/2}5d^4_{5/2}(J = 4)6s^1, J = 9/2$	
4	8.14	7.04	$72\%5d^4_{3/2}5d^4_{5/2}(J = 4)6s^1, J = 7/2$	$+23\%5d^3_{3/2}5d^5_{5/2}(J = 3)6s^1, J = 7/2$
5	8.65	7.75	$75\%5d^4_{3/2}5d^4_{5/2}(J = 2)6s^1, J = 5/2$	$+18\%5d^3_{3/2}5d^5_{5/2}(J = 3)6s^1, J = 5/2$
6	8.90	7.93	$73\%5d^4_{3/2}5d^4_{5/2}(J = 2)6s^1, J = 3/2$	$+17\%5d^3_{3/2}5d^5_{5/2}(J = 2)6s^1, J = 3/2$
7	9.64	8.41	$61\%5d^3_{3/2}5d^5_{5/2}(J = 3)6s^1, J = 5/2$	$+24\%5d^4_{3/2}5d^4_{5/2}(J = 2)6s^1, J = 5/2$
8	9.78	8.62	$77\%5d^3_{3/2}5d^5_{5/2}(J = 3)6s^1, J = 7/2$	$+23\%5d^4_{3/2}5d^4_{5/2}(J = 4)6s^1, J = 7/2$
9	10.19	9.37	$40\%5d^3_{3/2}5d^5_{5/2}(J = 2)6s^1, J = 3/2$	$+30\%5d^3_{3/2}5d^5_{5/2}(J = 1)6s^1, J = 3/2$
10	10.43	9.50	$60\%5d^4_{3/2}5d^4_{5/2}(J = 0)6s^1, J = 1/2$	$+21\%5d^3_{3/2}5d^5_{5/2}(J = 1)6s^1, J = 1/2$
11	10.63	9.67	$81\%5d^3_{3/2}5d^5_{5/2}(J = 2)6s^1, J = 5/2$	$+17\%5d^3_{3/2}5d^5_{5/2}(J = 3)6s^1, J = 5/2$
12	10.96	10.14	$64\%5d^3_{3/2}5d^5_{5/2}(J = 1)6s^1, J = 3/2$	$+20\%5d^3_{3/2}5d^4_{5/2}(J = 2)6s^1, J = 1/2$
13	11.43	10.63	$92\%5d^3_{3/2}5d^5_{5/2}(J = 4)6s^1, J = 9/2$	
		10.74	$95\%5d^3_{3/2}5d^5_{5/2}(J = 4)6s^1, J = 7/2$	
14	11.85	10.98	$77\%5d^3_{3/2}5d^5_{5/2}(J = 1)6s^1, J = 1/2$	$+18\%5d^4_{3/2}5d^4_{5/2}(J = 0)6s^1, J = 1/2$
15	12.40	11.33	$91\%5d^2_{3/2}(J = 2)5d^6_{5/2}6s^1, J = 5/2$	
		11.43	$56\%5d^2_{3/2}(J = 2)5d^5_{5/2}6s^1, J = 3/2$	$+37\%5d^3_{3/2}5d^5_{5/2}(J = 2)6s^1, J = 3/2$
16	15.42			
17	16.14	15.18	$77\%5d^2_{3/2}(J = 0)5d^6_{5/2}6s^1, J = 1/2$	$+22\%5d^4_{3/2}5d^4_{5/2}(J = 0)6s^1, J = 1/2$
18	16.49			
19	17.52			
20	18.07	16.80	$85\%5d^4_{3/2}5d^3_{5/2}(J = 9/2)6s^2, J = 9/2$	$+22\%5d^3_{3/2}5d^4_{5/2}(J = 4)6s^2, J = 9/2$
21	19.04			
22	19.25			
23	19.86	18.42	$79\%5d^3_{3/2}5d^4_{5/2}(J = 4)6s^2, J = 7/2$	$+15\%5d^3_{3/2}5d^4_{5/2}(J = 2)6s^2, J = 7/2$
24	20.34	18.66	$82\%5d^4_{3/2}5d^3_{5/2}(J = 3/2)6s^2, J = 3/2$	$+7\%5d^3_{3/2}5d^4_{5/2}(J = 0)6s^1, J = 3/2$
			$58\%5d^4_{3/2}5d^3_{5/2}(J = 5/2)6s^2, J = 5/2$	$+15\%5d^2_{3/2}(J = 2)5d^5_{5/2}6s^2, J = 5/2$
25	20.77			
26	21.25	19.61	$70\%5d^3_{3/2}5d^4_{5/2}(J = 2)6s^2, J = 3/2$	$+11\%5d^3_{3/2}5d^4_{5/2}(J = 0)6s^2, J = 3/2$
		19.81	$70\%5d^3_{3/2}5d^4_{5/2}(J = 4)6s^2, J = 5/2$	$+14\%5d^4_{3/2}5d^3_{5/2}(J = 5/2)6s^2, J = 5/2$
		19.89	$82\%5d^3_{3/2}5d^4_{5/2}(J = 4)6s^2, J = 9/2$	$+15\%5d^4_{3/2}5d^3_{5/2}(J = 9/2)6s^2, J = 9/2$
27	21.55	20.48	$93\%5d^3_{3/2}5d^4_{5/2}(J = 2)6s^2, J = 1/2$	
28	22.08	20.84	$100\%5d^3_{3/2}5d^4_{5/2}(J = 4)6s^2, J = 11/2$	
29	22.42	21.09	$68\%5d^3_{3/2}5d^4_{5/2}(J = 2)6s^2, J = 7/2$	$+28\%5d^2_{3/2}(J = 2)5d^5_{5/2}6s^2, J = 7/2$
30	23.05			
31	23.77	21.79	$78\%5d^2_{3/2}(J = 2)5d^5_{5/2}6s^2, J = 3/2$	$+13\%5d^3_{3/2}5d^4_{5/2}(J = 2)6s^2, J = 3/2$
		21.85	$60\%5d^2_{3/2}(J = 2)5d^5_{5/2}6s^2, J = 5/2$	$+17\%5d^3_{3/2}5d^4_{5/2}(J = 4)6s^2, J = 5/2$
32	26.18	22.59	$96\%5d^2_{3/2}(J = 2)5d^5_{5/2}6s^2, J = 9/2$	
		22.62	$76\%5d^3_{3/2}5d^4_{5/2}(J = 2)6s^2, J = 5/2$	$+15\%5d^4_{3/2}5d^3_{5/2}(J = 5/2)6s^2, J = 5/2$
		22.71	$93\%5d^2_{3/2}(J = 2)5d^5_{5/2}6s^2, J = 1/2$	
33	27.22	23.73	$65\%5d^2_{3/2}(J = 2)5d^5_{5/2}6s^2, J = 7/2$	$+17\%5d^3_{3/2}5d^4_{5/2}(J = 2)6s^2, J = 7/2$
		23.84	$43\%5d^1_{3/2}5d^6_{5/2}6s^2, J = 3/2$	$+32\%5d^3_{3/2}5d^4_{5/2}(J = 0)6s^2, J = 3/2$
34	28.60	26.09	$50\%5d^3_{3/2}5d^4_{5/2}(J = 0)6s^2, J = 3/2$	$+46\%5d^1_{3/2}5d^4_{5/2}6s^2, J = 3/2$
		26.69	$78\%5d^2_{3/2}(J = 0)5d^5_{5/2}6s^2, J = 5/2$	$+10\%5d^2_{3/2}(J = 2)5d^5_{5/2}6s^2, J = 5/2$

$5d^7 6s^2$ to be the spin-orbit split $5d^9$ in the isoelectronic series of Ir I to Pt II, Au III, and Hg IV has been already demonstrated by Joshi *et al.* [20] who reported 1.94 eV for the spin-orbit splitting as being almost an exact match to our observation.

Our relativistic calculation predicts the energy separation between configuration groups $5d^9$, $5d^8 6s^1$, and $5d^7 6s^2$ quite well. The distribution of the states in the main part of the $5d^8 6s^1$ (peaks 3–17 in Table I) configuration are nicely predicted. The experimental energy separations for peaks 3–16 agree within about 50 meV with the line separations given by van der Valk *et al.* [21] except for line number 14, where we have fitted a 270 meV higher separation to the lowest state. This may be due to the fitting procedure of the small ($J = 1/2$) state. Our *ab initio* prediction provides the same total J assignment for most of the states as the semiempirical approach used in the previous work. Only the very closely located states 9 and 10 seem to be in different order in respect to each other. According to our predictions these are the states with the least percentage of the leading $J\,J$ term. In addition, our fitting has provided only one line to the close-lying predicted pairs of states in peaks 13 and 15. The predicted order of appearance seems to be changed for both of these pairs as well, in comparison to Ref. [21]. In addition, our prediction also suggests the appearance of line 17, observed experimentally 16.14 eV above the Hg^{3+} ground state. Our calculation predicts the $5d^7 6s^2$ triply ionized states to lie around 75–87 eV binding energies. The very good energy and statistical intensity matching of the earlier structures encouraged us to give assignments for the main lines in the $5d^7 6s^2$ group obviously visible at the experimental binding energies of 80–90 eV. No reports on the optically observed values for the binding energies or the line separations of these states were found to exist. Instead of single states, the region is covered with several slightly separated groups of many lines which, however, prevent individual assignments and thus Table I provides only a tentative understanding of the distribution in this group.

The quadruply ionized states presented in Fig. 4 were measured at a photon energy of 180 eV. The relative number of four-electron events is low due to the absence of any direct cascade decay channels before the $4d^{-1}$ initial hole at the binding energy of 366 eV [14]. The calculated energy positions of the Hg^{4+} states are presented as vertical bars in Fig. 4. The length of the bars again presents the $2J + 1$ statistical weights as estimates of the intensity distributions within each final state group defined by the configuration. The identifications of the Hg^{4+} states are less clear than those of doubly and triply ionized states. The first experimental group of states between 110 and 120 eV experimental binding energies is still relatively well matched to our prediction with nine calculated $5d^8$ states, but already the second $5d^7 6s$, and especially the third $5d^6 6s^2$ predicted groups, are an admixture of high numbers of states, preventing any individual state identifications. The Hg^{4+} threshold is, however, directly determined to be at 112.2 eV ±150 meV, and the $5d^8$ states are located at 110–120 eV binding energies. The binding energies for these six experimentally obtained $5d^8$ states are given in Table II, together with predicted identifications from calculations. In the case of $5d^8$ states of Hg^{4+} we also present a detailed comparison of the experimental findings to the high resolution state distributions obtained by optical spectroscopy [22] to emphasize the differences from our experiments. In comparison to the work by Raassen *et al.* [22], our reported energies for states are less accurate, however directly providing the binding energies of the states. The predicted assignments for the lines seem to match well on total J. For state distributions, the states 2 and 3 with $J = 2$ and $J = 3$ do have equal energy separation within our reported accuracy with the optical data. The following four relatively closely lying states have been fitted as two structures only (peaks 4 and 5), thus no proper further comparison to Raassen *et al.* [22] is possible, although the results are in line with their report on the energy distribution. Our relativistic prediction would suggest that the order of these $J = 2$ and $J = 0$ states is reversed in comparison to the assignment in the previous work [22].

Wyart *et al.* [23] have also presented the assignments and energy distributions based on the optical data and semiempirical least-square-fitted Hartree-Fock calculations for the states of $5d^7 6s^1$ configuration. The quality of our data does not allow for a detailed comparison but suggests that the first state of

TABLE II. Experimental and calculated binding energies and identification of quadruply ionized states of Hg. All binding energies are given taken Hg^{4+} threshold (peak number 1) as reference.

	Binding energies (eV)				Identification	
Peak	Expt.	Ref. [22][a]	Calc.	Ref. [22]	Calc.	
1	112.2 ± 0.15	0	105.8	$^3F_4$	$93\%5d^4_{3/2}5d^4_{5/2}, J=4$	$+7\%5d^3_{3/2}5d^5_{5/2}, J=4$
2	1.1	0.930 66	1.2	$^1D_2$	$91\%5d^4_{3/2}5d^4_{5/2}, J=2$	$+5\%5d^3_{3/2}5d^5_{5/2}, J=2$
3	2.0	1.863 22	1.7	$^3F_3$	$100\%5d^3_{3/2}5d^5_{5/2}, J=3$	
4	2.9	2.5750	2.7	$^3P_0$	$77\%5d^3_{3/2}5d^5_{5/2}, J=2$	$+15\%5d^2_{3/2}5d^6_{5/2}, J=2$
		2.695 45	3.1	$^3P_2$	$76\%5d^4_{3/2}5d^4_{5/2}, J=0$	$+23\%5d^2_{3/2}5d^6_{5/2}, J=0$
5	3.8	3.167 47	3.4	$^3P_1$	$98\%5d^3_{3/2}5d^5_{5/2}, J=1$	
		3.682 29	4.0	$^1G_4$	$92\%5d^3_{3/2}5d^5_{5/2}, J=4$	$+7\%5d^4_{3/2}5d^4_{5/2}, J=4$
6	4.8	4.5709	4.5	$^3F_2$	$82\%5d^2_{3/2}5d^6_{5/2}, J=2$	$+17\%5d^3_{3/2}5d^5_{5/2}, J=2$
7			8.6	$^1S_0$	$75\%5d^2_{3/2}5d^6_{5/2}, J=0$	$+24\%5d^4_{3/2}5d^4_{5/2}, J=0$

[a]Binding energies converted to eV from cm^{-1} values reported in Ref. [22].

$5d^7 6s^1$ lies at 122.7 eV binding energy. Our predictions also suggest a $5d^6 s^2$ configuration to lie at around 130–140 eV binding-energy regions. However, no intensity was found to populate these states at the photon energy of 180 eV.

V. CONCLUSION

Multielectron coincidence spectroscopy has been successfully used with synchrotron radiation excitation to study the multiply ionized states of vapor phase mercury. Relativistic multielectron calculations together with statistical intensity distributions have been used to predict the spectral states. The results demonstrate the ability of multielectron spectroscopy to directly provide information on multiply ionized states of metal vapors. The experimental information obtained on the binding energies of triply ionized, and especially quadruply ionized states, is spectral information which complements the present data tabulated in Moore's [19] tables and connects the individual state distributions obtained by Joshi *et al.* [20], Van der Valk *et al.* [21], Raassen *et al.* [22], and Wyart *et al.* [23] to the absolute binding-energy scale. Relativistic calculations applying the GRASP code package have proved to be a useful tool in the interpretation of such heavy metal spectra, as they predict the energy distributions of ionized states in fair agreement with the experimental data. Although the processes populating the final states (involving $4f$ inner-shell ionization) were not considered, as a first approximation, statistical intensity distribution within each final-state configuration was found to be in good agreement with observations.

ACKNOWLEDGMENTS

This work has been financially supported by the Research Council for Natural Sciences of the Academy of Finland and the European Community-Research Infrastructure Action under the FP6 "Structuring the European Research Area" Programme (through the Integrated Infrastructure Initiative "Integrating Activity on Synchrotron and Free Electron Laser Science"). The help of Henri Tikkala in the data tabulation is also acknowledged.

[1] K. Siegbahn *et al.*, *ESCA Atomic, Molecular and Solid State Structure Studied by Means of Electron Spectroscopy*, Nova Acta Regiae Societatis Scientiarum Upsaliensis Series IV, Vol. 20 (Almqvist & Wiksells Boktryckeri AB, Uppsala, 1967).

[2] See, for example, D. W. Turner *et al.*, J. Chem. Phys. **45**, 471 (1966); Proc. R. Soc. London, Ser. A **307**, 15 (1968).

[3] J. H. D. Eland, O. Vieuxmaire, T. Kinugawa, P. Lablanquie, R. I. Hall, and F. Penent, Phys. Rev. Lett. **90**, 053003 (2003).

[4] F. Penent, J. Palaudoux, P. Lablanquie, L. Andric, R. Feifel, and J. H. D. Eland, Phys. Rev. Lett. **95**, 083002 (2005).

[5] P. Lablanquie, L. Andric, J. Palaudoux, U. Becker, M. Braune, J. Viefhaus, J. H. D. Eland, and F. Penent, J. Electron Spectrosc. Relat. Phenom. **156**, 51 (2007).

[6] J. Palaudoux, P. Lablanquie, L. Andric, K. Ito, E. Shigemasa, J. H. D. Eland, V. Jonauskas, S. Kucas, R. Karazija, and F. Penent, Phys. Rev. A **82**, 043419 (2010).

[7] E. Andersson, S. Fritzsche, P. Linusson, L. Hedin, J. H. D. Eland, J.-E. Rubensson, L. Karlsson, and R. Feifel, Phys. Rev. A **82**, 043418 (2010).

[8] P. Lablanquie *et al.*, Phys. Rev. Lett. **106**, 063003 (2011).

[9] J. H. D. Eland, M. Tashiro, P. Linusson, M. Ehara, K. Ueda, and R. Feifel, Phys. Rev. Lett. **105**, 213005 (2010).

[10] J. H. D. Eland, R. Feifel, and D. Edvardsson, J. Phys. Chem. A **108**, 9721 (2004).

[11] K. J. Ross and B. Sonntag, Rev. Sci. Instrum. **66**, 4409 (1995).

[12] S. Aksela, M. Harkoma, and H. Aksela, Phys. Rev. A **29**, 2915 (1984).

[13] M. Huttula, L. Partanen, A. Mäkinen, T. Kantia, H. Aksela, and S. Aksela, Phys. Rev. A, **79**, 023412 (2009).

[14] S. Svensson, N. Mårtensson, E. Basilier, P. Å. Malmquist, U. Gelius, and K. Siegbahn, J. Electron. Spectrosc. Relat. Phenom. **9**, 51 (1975).

[15] P. H. Kobrin, P. A. Heimann, H. G. Kerkhoff, D. W. Lindle, C. M. Truesdale, T. A. Ferret, U. Becker, and D. A. Shirley, Phys. Rev. A **27**, 3031 (1983).

[16] H. Aksela, S. Aksela, J. S. Jen, and T. D. Thomas, Phys. Rev. A **15**, 985 (1977).

[17] R. B. Cairns, H. Harrison, and R. I. Schoen, J. Chem. Phys. **53**, 96 (1970).

[18] J. H. D. Eland and R. Feifel, J. Phys. Chem. A **108**, 9721 (2004).

[19] C. E. Moore, *Atomic Energy Levels*, US Natl. Bur. Stand. (US GPO, Washington, D.C., 1971), Vol. 1.

[20] Y. N. Joshi, A. J. J. Raassen, and B. Arcimowicz, J. Opt. Soc. Am. B **6**, 534 (1989).

[21] A. A. van der Valk, A. A. Raassen, and Y. N. Joshi, J. Opt. Soc. Am. B **7**, 1182 (1990).

[22] A. J. J. Raassen, Y. N. Joshi, and A. Tauheed, Phys. Scr. **43**, 44 (1991).

[23] J.-F. Wyart, A. J. J. Raassen, G. J. van het Hof, and Y. N. Joshi, Phys. Scr. **47**, 784 (1993).

[24] Y. Hikosaka, P. Lablanquie, F. Penent, T. Kaneyasu, E. Shigemasa, R. Feifel, J. H. D. Eland, and K. Ito, Phys. Rev. Lett. **102**, 013002 (2009).

[25] K. Ito, F. Penent, Y. Hikosaka, E. Shigemasa, I. H. Suzuki, J. H. D. Eland, and P. Lablanquie, Rev. Sci. Instrum. **80**, 123101 (2009).

[26] F. A. Parpia, C. F. Fischer, and I. P. Grant, Comput. Phys. Commun. **94**, 249 (1996).

[27] S. Fritzsche, J. Electron Spectrosc. Relat. Phenom. **114**, 1155 (2001).

[28] S. Fritzsche, C. F. Fischer, and I. P. Grant, Comput. Phys. Commun. **124**, 340 (2000).

[29] P. Lablanquie *et al.* (unpublished).

[30] Y. Ralchenko, A. E. Kramida, J. Reader, and NIST ADV Team (2008), NIST Atomic Spectra Database (version 3.1.5), [http://physics.nist.gov/asd3/] (National Institute of Standards and Technology, Gaithersburg, MD, 2010).